Characterization of Voltage Instrument Transformers Under Nonsinusoidal Conditions Based on the Best Linear Approximation

Marco Faifer, *Senior Member, IEEE*, Christian Laurano, *Student Member, IEEE*, Roberto Ottoboni, *Fellow, IEEE*, Sergio Toscani, *Member, IEEE*, and Michele Zanoni, *Student Member, IEEE*

***Abstract*— Voltage instrument transformers are usually tested at the rated frequency. In order to assess their performance in measuring harmonic components, typically, the frequency response function (FRF) is evaluated. Therefore, this conventional characterization does not consider nonlinear effects that may have a nonnegligible impact on the accuracy, especially when the transducer under test is represented by an inductive voltage transformer (VT). In this paper, a simple procedure for the characterization of voltage instrument transformers is presented. The method is based on the concept of best linear approximation of a nonlinear system. It requires applying a class of excitation signals that resembles the typical voltage waveforms found in power systems. Results consist of the FRF that permits the best linear compensation of the transducer response, and sample variances that allow quantifying the impact of noise and nonlinearities on the accuracy. The method is presented and explained by means of numerical simulations. After that, it has been applied to the characterization of a conventional inductive VT. Experimental results show how the accuracy of the transducer under test is heavily degraded by nonlinear phenomena when low-order voltage harmonics are considered.**

***Index Terms*— Calibration, frequency-domain analysis, frequency response, instrument transformers, measurement uncertainty, nonlinear systems, power system harmonics, voltage measurement, voltage transformers (VTs).**

I. Introduction

THE number of nonlinear loads and generators connected to distribution networks has increased dramatically in the last decade, thus producing a considerable growth of the voltage harmonic distortion. For this reason, voltage quality monitoring has become more and more important and ruled by specific standards. In particular, [1] suggests techniques and accuracy requirements for harmonics and interharmonics measurements. Of course, this demands for voltage transducers with adequate performance [2]–[7], thus capable of accurately measure harmonic amplitudes and phases. Instrument transformers are conventionally calibrated and characterized at their rated frequency [8]; their metrological performance is expressed in terms of accuracy class, corresponding to ratio and phase angle error limits.

On the other hand, low-power instrument transformers are ruled by [9] that specifies ratio and phase error limits for every harmonic order and standard accuracy class. As for their metrological characterization, [9] states that the test signal should also include the fundamental term at the rated voltage and frequency, other than the harmonic components. The aim is to consider nonlinear effects such as harmonic distortion and intermodulation. Since similar tests require a somewhat more complex experimental setup, including a voltage generator [10], [11] capable of injecting complex test signals, the standard [9] allows testing instrument transformers by applying a signal containing just one single spectral component at once. However, it is clear that this procedure is unable to capture the actual performance of the transducer when nonlinear effects are not negligible.

Technical report [12] discusses the employment of different types of instrument transformers for power quality measurement, and in particular for harmonic voltage monitoring. Even in this case, it is stated that when the behavior of the transducer is likely to be affected by the presence of the fundamental component, tests should be performed by applying voltages containing a main component having rated amplitude and frequency, other than (small) harmonics, subharmonics, or interharmonics. It should be stressed that the impact of nonlinearities on harmonic voltage measurement is exacerbated by the large ratio between the magnitude of the fundamental and those of the other spectral components.

A typical example of transducer that may exhibit significant nonlinearities is represented by the conventional voltage transformer (VT). Many papers report frequency response measurements [13]–[16], but [12] warns to pay special attention on the employed method, since it may significantly affect the results because of nonlinear phenomena. Only few works [17], [18] mention the potential impact of such nonlinearities.

A proper characterization of voltage instrument transformers devoted to harmonic measurements should include and quantify nonlinearities, which in principle cannot be decoupled from the dynamic behavior. A first possibility is to design

Manuscript received November 9, 2017; revised February 8, 2018; accepted February 9, 2018. Date of publication March 29, 2018; date of current version September 17, 2018. The Associate Editor coordinating the review process was Dr. Carlo Muscas. *(Corresponding author: Sergio Toscani.)*

The authors are with the Dipartimento di Elettronica, Informazione e Bioingegneria, Politecnico di Milano, 20133 Milan, Italy (e-mail: marco.faifer@polimi.it; christian.laurano@polimi.it; roberto.ottoboni@polimi.it; sergio.toscani@polimi.it; michele.zanoni@polimi.it).

a testing procedure based on a nonlinear model, for example, using the Volterra approach [19], [20], which represents the straightforward extension of the linear time invariant system theory. The main drawback is represented by the huge complexity of the model even considering few input harmonics and low nonlinearity order. A simplified approach specifically developed for the modeling of power system components [21], [22] can be employed. It allows considerably reducing the model complexity without noticeably decreasing performance.

A second approach is to adopt a different method [23] that is still based on a linear modeling of the instrument transformer: evaluating the best linear approximation (BLA) [24]–[28]. By applying a set of realistic voltage waveforms to the transducer under test, the BLA is defined as the frequency response function (FRF) which guarantees the best frequency-domain reconstruction of the measured voltage from the transducer output. Nonlinear effects produce mismatch between the actual transducer input and that predicted from the output by using the BLA. Random noise appears as the standard deviation of the transducer output spectrum during each test realization.

The proposed procedure is briefly explained and applied using numerical simulations. After that, the method is employed for the characterization of a conventional voltage instrument transformer. Experimental results are reported and deeply discussed.

II. Framework

As discussed during the introduction, the accuracy of an instrument transformer in measuring harmonic voltages is typically assessed by identifying its FRF. This is performed by applying known sinewaves at different frequencies and measuring the output spectral component having the same frequency as the input. Of course, this representation is exact only if the transducer is a linear time invariant system, but all transducers are nonlinear to some extent. In this case, undermodeling effects arise: a physical system is represented with an approximated model which is not capable to fully explain its behavior, thus introducing definitional uncertainty.

Undermodeling appears as a dependence of the identified model on the stimulus signal employed for its estimation. Therefore, it becomes clear that in this case, the instrument transformer should be tested by applying voltage waveforms similar to those typically found during its normal operation.

For this reason, a class E of excitation signals is introduced. It consists of periodic multisine voltages $v_1^{[m]}(t)$ having a fundamental frequency f_0 (and angular frequency ω_0) and a maximum harmonic order N. The generic time-domain expression of each signal belonging to E is

$$v_1^{[m]}(t) = \sqrt{2}\sum_{k=0}^{N} \Re\left[V_1^{[m]}(jk\omega_0)e^{jk\omega_0 t}\right] \tag{1}$$

where $V_1^{[m]}(jk\omega_0)$ is the kth order harmonic phasor. Its magnitude and phase can be considered as realizations of independently distributed random processes. Their probability density functions (PDFs) should be selected in order to obtain the typical voltage spectra found in distribution systems.

TABLE I
Harmonic Voltage Amplitude Limits MV/LV Grids (Percentages of the Fundamental Component)

Odd Harmonics				Even Harmonics	
k	P_k	k	P_k	k	P_k
3	5.0 %	15	0.5 %	2	2.0 %
5	6.0 %	17	2.5 %	4	1.0 %
7	5.0%	19	1.5 %	6	0.5 %
9	1.5 %	21	0.5 %	8	0.5 %
11	3.5 %	23	1.5 %	10	0.5 %
13	3.0 %	25	1.5 %	14÷24	0.5 %

For this purpose, Standard EN 50160 [29] defines the limits for harmonic voltages up to the 25th order applicable to public medium-voltage (MV) and low-voltage (LV) distribution networks (Table I). By considering a one-week observation period, the 10-min average root-mean-square value of each harmonic should be below the corresponding limit for 95% of the time. Moreover, it states that the 10-min average root-mean-square voltage should be within 90% and the 110% of the rated value V_n for 95% of the time.

Hence, these values P_k can be used as 95th percentiles of the PDFs employed to generate the harmonic amplitudes. However, the standard does not provide information about the shapes of their PDFs, nor about the harmonic phases.

III. Voltage Instrument Transformer Characterization Based on the Best Linear Approximation

Let us suppose that it is possible to feed the instrument transformer under test with known, multisine voltages $v_1^{[m]}$ belonging to the previously defined class E. Let us introduce the corresponding transducer outputs $v_2^{[m]}$, and the transducer input and output spectra $V_1^{[m]}(jk\omega_0)$ and $V_2^{[m]}(jk\omega_0)$, respectively. Let us define the measured voltage spectra $V_{1,m}^{[m]}(jk\omega_0)$, obtained from $V_2^{[m]}(jk\omega_0)$. For a given signal, a synthetic index to evaluate the frequency-domain metrological performance of the transducer is represented by the total vector error (TVE)

$$\mathrm{TVE}^{[m]}(jk\omega_0) = \left|V_1^{[m]}(jk\omega_0) - V_{1,m}^{[m]}(jk\omega_0)\right|. \tag{2}$$

It corresponds to the distance in the complex plane between the actual and the measured voltage harmonic phasors. For a given set of M excitation voltages $V_1^{[m]}(jk\omega_0)$ belonging to the class E defined in Section II, the BLA $G_{\mathrm{BLA}}(jk\omega_0)$ of the transducer under test is defined as the FRF that when applied to its output, minimizes the mean square TVE. In terms of equations

$$G_{\mathrm{BLA}}(jk\omega_0) = \arg\min_{G(jk\omega_0)} \|\mathbf{V}_1(jk\omega_0) - G(jk\omega_0)\mathbf{V}_2(jk\omega_0)\| \tag{3}$$

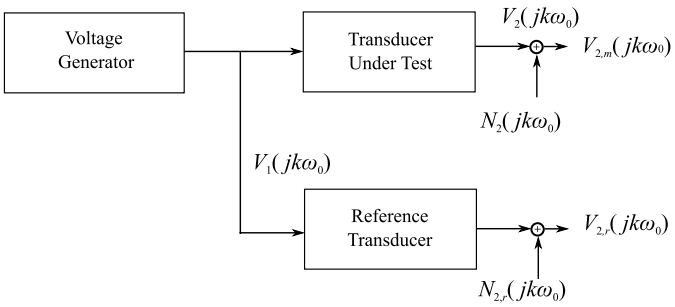

Fig. 1. Block diagram of the test setup.

where

$$\mathbf{V}_2(jk\omega_0) = \begin{bmatrix} V_2^{[1]}(jk\omega_0) \\ \vdots \\ V_2^{[M]}(jk\omega_0) \end{bmatrix} \quad \mathbf{V}_1(jk\omega_0) = \begin{bmatrix} V_1^{[1]}(jk\omega_0) \\ \vdots \\ V_1^{[M]}(jk\omega_0) \end{bmatrix} \tag{4}$$

while $\| \ \|$ denotes the Euclidean norm. Solving (3) leads to

$$\tilde{G}_{\mathrm{BLA}}(jk\omega_0) = \frac{\mathbf{V}_2^H(jk\omega_0)\mathbf{V}_1(jk\omega_0)}{\|\mathbf{V}_2(jk\omega_0)\|^2} \tag{5}$$

where $^{\mathrm{H}}$ denotes the Hermitian transpose. Defining $S_{22}(jk\omega_0)$ and $S_{12}(jk\omega_0)$ as the auto and cross spectra, respectively,

$$\begin{aligned} S_{12}(jk\omega_0) &= \mathbf{V}_2^H(jk\omega_0)\mathbf{V}_1(jk\omega_0) \\ S_{22}(jk\omega_0) &= \|\mathbf{V}_2(jk\omega_0)\|^2. \end{aligned} \tag{6}$$

Equation (5) can be rewritten as

$$\tilde{G}_{\mathrm{BLA}}(j\omega) = \frac{S_{12}(jk\omega_0)}{S_{22}(jk\omega_0)}. \tag{7}$$

The excitation voltage $V_1(jk\omega_0)$ is measured by a reference transducer, characterized by negligible nonlinearity and an FRF $G_r(jk\omega_0)$ known with very low uncertainty. Therefore, $V_1(jk\omega_0)$ can be reconstructed from the reference transducer output $V_{2,r}(jk\omega_0)$ by using $G_r(jk\omega_0)$

$$V_{1,r}(jk\omega_0) = G_r(jk\omega_0)V_{2,r}(jk\omega_0) \approx V_1(jk\omega_0). \tag{8}$$

As for the transformer under test, the difference between the actual voltage $V_1(jk\omega_0)$ and its reconstruction performed by using the BLA results in a term $V_{\mathrm{NL}}(jk\omega_0)$ which depends on the transducer nonlinearity

$$V_1(jk\omega_0) = G_{\mathrm{BLA}}(jk\omega_0)V_2(jk\omega_0) + V_{\mathrm{NL}}(jk\omega_0). \tag{9}$$

A. Measurement Noise

In general, noise affects both the output of the reference transducer and that of the transducer under test. Fig. 1 shows the block diagram of the test setup used to estimate the BLA, highlighting the considered noise sources.

$N_2(jk\omega_0)$ and $N_{2,r}(jk\omega_0)$ are complex random variables that represent the impact of noise on the spectra of the transducer outputs. From Fig. 1, it is clear that

$$\begin{aligned} V_2(jk\omega_0) &= V_{2,m}(jk\omega_0) - N_2(jk\omega_0) \\ V_1(jk\omega_0) &= G_r(jk\omega_0)(V_{2,r}(jk\omega_0) - N_{2,r}(jk\omega_0)) \\ &= V_{1,r}\,(jk\omega_0) - N_r\,(jk\omega_0)\,. \end{aligned} \tag{10}$$

The two expressions of (10) can be substituted in (9), and the primary voltage measured by the reference transducer can be expressed as

$$V_{1,r}(jk\omega_0) = G_{\mathrm{BLA}}(jk\omega_0)V_2(jk\omega_0) + V_{\mathrm{NL}}(jk\omega_0) + N_r(jk\omega_0). \tag{11}$$

In turn, $V_{1,r}(jk\omega_0)$ can be split into three different contributions.

1) $G_{\mathrm{BLA}}(jk\omega_0)V_2(jk\omega_0)$ is the reconstruction of the excitation signal by using the BLA and the transducer output. It should be noticed that $G_{\mathrm{BLA}}(jk\omega_0)$ differs from the linear part of the input–output characteristic of the transducer, since it is biased by the systematic nonlinear contributions. This term is also affected by the measurement noise at the output of the transducer under test.
2) $V_{\mathrm{NL}}(jk\omega_0)$ is purely produced by undermodeling, containing the stochastic nonlinear contribution.
3) $N_r(jk\omega_0)$ represents the measurement noise at the output of the reference transducer.

B. Reducing the Impact of Noise

Measurement noise biases the estimated BLA and increases its variance. It is extremely important to apply averaging before computing the auto and cross spectra in order to reduce these detrimental effects.

Let us suppose that $N_2(jk\omega_0)$ and $N_{2,r}(jk\omega_0)$ have circular complex distribution, zero expectation, and second-order moments expressed by the respective covariance matrices. Furthermore, let us assume that noises are not correlated with voltages. Under these mild conditions, frequency domain averaging allows mitigating the impact of noise [24].

Let us acquire P periods of $v_{1,r}$ and v_2 for each generic mth test signal. $V_{1,r}^{[m,p]}(jk\omega_0)$ and $V_2^{[m,p]}(jk\omega_0)$ are their spectra computed on the pth period of the mth signal. The average spectra $\tilde{V}_{1,r}^{[m]}(jk\omega_0)$ and $\tilde{V}_2^{[m]}(jk\omega_0)$ can be evaluated as

$$\begin{aligned} \tilde{V}_{1,r}^{[m]}(jk\omega_0) &= \frac{1}{P}\sum_{p=1}^{P} V_{1,r}^{[m,p]}(jk\omega_0) \\ \tilde{V}_2^{[m]}(jk\omega_0) &= \frac{1}{P}\sum_{p=1}^{P} V_2^{[m,p]}(jk\omega_0). \end{aligned} \tag{12}$$

Once having computed $\tilde{V}_{1,r}^{[m]}(jk\omega_0)$ and $\tilde{V}_2^{[m]}(jk\omega_0)$ for each signal, $V_1(jk\omega_0)$ and $V_2(jk\omega_0)$ are replaced in (4) with $\tilde{V}_{1,r}(jk\omega_0)$ and $\tilde{V}_2(jk\omega_0)$ obtained by concatenating the M average spectra. Then, the auto and cross spectra can be evaluated using (6), and the BLA can be estimated

$$\tilde{G}_{\mathrm{BLA}}(jk\omega_0) = \frac{\tilde{S}_{1r2}(jk\omega_0)}{\tilde{S}_{22}(jk\omega_0)}. \tag{13}$$

C. FRF Variances

The target of the proposed procedure is not only evaluating the BLA of the transformer under test, but also detecting and quantifying stochastic nonlinearities that are not masked by the measurement noise.

For each pth period of the mth trial, it is possible to obtain an estimation of the FRF

$$\tilde{G}^{[m,p]}(jk\omega_0) = \frac{\tilde{S}_{1r2}^{[m,p]}(jk\omega_0)}{\tilde{S}_{22}^{[m,p]}(jk\omega_0)}. \tag{14}$$

The average value over the P periods of (14) for each mth trial is given by

$$\tilde{G}^{[m]}(jk\omega_0) = \frac{1}{P}\sum_{p=1}^{P} \tilde{G}^{[m,p]}(jk\omega_0). \tag{15}$$

By definition, the excitation signal is periodic. Therefore, supposing that the system is time invariant while excluding complex nonlinear behavior (limit cycles, chaos, etc.), the response is periodic having the same period as the input. Hence, under this assumption, the variance $s_{G,m}^2(jk\omega_0)$ of the FRF evaluated by considering the P periods acquired for the mth test signal is purely due to noise

$$s_{G,m}^2(jk\omega_0) = \frac{1}{P(P-1)}\sum_{p=1}^{P} |\tilde{G}^{[m,p]}(jk\omega_0) - \tilde{G}^{[m]}(jk\omega_0)|^2. \tag{16}$$

The sample variance (16) can also be directly estimated by using the variances of the spectra $\tilde{V}_{1,r}^{[m]}(jk\omega_0)$ and $\tilde{V}_2^{[m]}(jk\omega_0)$ of the mth realization

$$\begin{aligned} s_{G,m}^2(jk\omega_0) = {} & |\tilde{G}^{[m]}(jk\omega_0)|^2 \\ & \cdot \left[\frac{s_{1,m}^2(jk\omega_0)}{\left|\tilde{V}_{1,r}^{[m]}(jk\omega_0)\right|^2} + \frac{s_{2,m}^2(jk\omega_0)}{\left|\tilde{V}_2^{[m]}(jk\omega_0)\right|^2} \right. \\ & \left. -2\Re\left(\frac{s_{12,m}^2(jk\omega_0)}{\tilde{V}_{1,r}^{[m]}(jk\omega_0)\left(\tilde{V}_2^{[m]}(jk\omega_0)\right)^*} \right) \right]. \end{aligned} \tag{17}$$

$*$ denotes the complex conjugate operation, and $s_{1,m}^2(jk\omega_0)$, $s_{2,m}^2(jk\omega_0)$, and $s_{12,m}^2(jk\omega_0)$ are the variances and covariance of $\tilde{V}_{1,r}(jk\omega_0)$ and $\tilde{V}_2(jk\omega_0)$ evaluated by considering the P periods of the mth trial

$$\begin{aligned} s_{1,m}^2(jk\omega_0) &= \frac{1}{P(P-1)}\sum_{p=1}^{P} \left| V_{1,r}^{[m,p]}(jk\omega_0) - \tilde{V}_{1,r}^{[m]}(jk\omega_0) \right|^2 \\ s_{2,m}^2(jk\omega_0) &= \frac{1}{P(P-1)}\sum_{p=1}^{P} \left| V_2^{[m,p]}(jk\omega_0) - \tilde{V}_2^{[m]}(jk\omega_0) \right|^2 \\ s_{12,m}^2(jk\omega_0) &= \frac{1}{P(P-1)}\sum_{p=1}^{P} \left(V_{1,r}^{[m,p]}(jk\omega_0) - \tilde{V}_{1,r}^{[m]}(jk\omega_0) \right) \\ &\quad \cdot \left(V_2^{[m,p]}(jk\omega_0) - \tilde{V}_2^{[m]}(jk\omega_0) \right)^*. \end{aligned} \tag{18}$$

Finally, the noise variance of the BLA $s_{\mathrm{BLA},N}^2(jk\omega_0)$ can be obtained as the mean of (16) when all the M tests are considered. It quantifies the impact of random noise on the estimated BLA

$$s_{\mathrm{BLA},N}^2(jk\omega_0) = \frac{1}{M^2}\sum_{m=1}^{M} s_{G,m}^2(jk\omega_0). \tag{19}$$

Equation (15) allows obtaining an FRF estimation for each test signal. When considering all the M trials, the FRFs are in general different because of two effects: measurement noise and nonlinearities. In fact, unmodeled nonlinearities produce a dependence of the evaluated FRF $\tilde{G}^{[m]}(jk\omega_0)$ on the specific mth excitation signal. Such stochastic behavior can be quantified by using the M FRF estimations to compute $s_{\mathrm{BLA}}^2(jk\omega_0)$, namely, the total sample standard deviation of the BLA

$$s_{\mathrm{BLA}}^2(jk\omega_0) = \frac{1}{M(M-1)}\sum_{m=1}^{M} |\tilde{G}^{[m]}(jk\omega_0) - \tilde{G}_{\mathrm{BLA}}(jk\omega_0)|^2. \tag{20}$$

D. Variance Analysis

Once having computed the aforementioned variances, the impact of the transducer nonlinearity can be assessed. Actually, the sample variance $s_{\mathrm{BLA},N}^2$ defined by (19) quantifies the variability of the BLA due to noise; basically, it can be considered as an A-type evaluation of the standard uncertainty of the BLA due to noise. On the other hand, the variance s_{BLA}^2 introduced by (20) takes into account both noise and (stochastic) nonlinear contributions. Therefore, it represents an A-type uncertainty evaluation of the BLA that considers the effects of noise and definitional uncertainty due to undermodeling.

During the testing of the instrument transformer, both variances have to be evaluated. Two different scenarios may occur

$$\begin{aligned} &\text{I.} \quad s_{\mathrm{BLA}}^2 \approx s_{\mathrm{BLA},N}^2 \\ &\text{II.} \quad s_{\mathrm{BLA}}^2 \gg s_{\mathrm{BLA},N}^2. \end{aligned} \tag{21}$$

In the first case, for the class E of excitation signals, the nonlinear contribution to the total sample variance is masked by noise. Then, in order to detect possible nonlinearities, it is mandatory to reduce the impact of noise, for example, by increasing the number P of acquired periods or by improving the measurement setup, having assumed that the main noise source is not represented by the transducer under test.

Conversely, if the two variances are significantly different, it means that the transducer nonlinearities are relevant with respect to the noise floor. In this case, the total variance s_{BLA}^2 does not drop significantly by increasing the number P of acquired periods.

IV. Numerical Simulations

In order to better explain the proposed procedure described in Section III, it has been applied through numerical simulations to the testing of a conventional inductive VT [23]. In this way, the impact of measurement noise can be highlighted.

The VT has been represented with the usual Steinmetz equivalent circuit, as reported in Fig. 2. The values of the resistances, of the leakage inductances, and of the turn ratio are reported in Table II; the nonlinear magnetizing inductance L_m is characterized by the single-valued flux linkage–current relation shown in Fig. 3. The input signal is supposed to be measured with an ideal transducer.

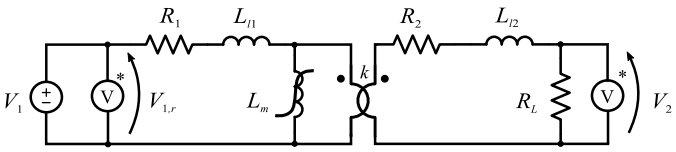

Fig. 2. Equivalent circuit of the VT.

TABLE II
VT PARAMETERS

V_{n1} [V]	k	R_1 [Ω]	R_2 [Ω]	L_{l1} [mH]	L_{l2} [mH]	R_L [Ω]
200	2	6	1.25	4.75	1.19	1600

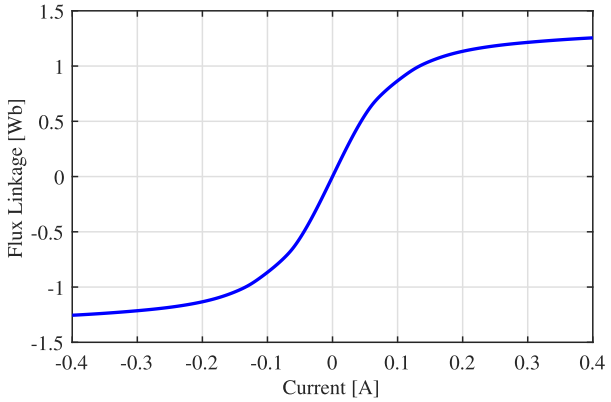

Fig. 3. Flux linkage–current characteristic of the magnetizing inductance.

A. Excitation Signals

As stated by [30], mainly because of resonances due to winding capacitances, VTs are typically suitable for measuring harmonic components having frequencies up to around 1 kHz, even if this value may change considerably according to voltage level and construction. Therefore, voltage harmonics up to the 25th order for a 50-Hz system have been considered in this paper.

From Section IV, it is clear that the excitation signals employed to estimate the BLA should be as close as possible to those found in typical working conditions. For this reason, the class E of excitation signals has been defined starting from the 95th percentile values for the root-mean-square amplitudes prescribed by the standard EN 50160. However, the standard does not provide information about the shape of their PDFs, nor about the phases: some assumptions have to be introduced. Therefore, the fundamental amplitude is supposed to be normally distributed, having a mean value equal to the rated voltage and a standard deviation so that it falls between $\pm 10\%$ of the rated value with 95% probability. Harmonic phasors are supposed to follow zero mean, circular complex normal distributions, resulting in uncorrelated, normally distributed real and imaginary parts. Under this hypothesis, harmonic amplitudes follow Rayleigh distributions characterized by σ parameters that can be easily computed from the 95th percentiles reported in Table I, while the phases are independent and uniformly distributed in the interval $[-\pi, \pi]$.

B. Simulation Results

The VT characterization has been simulated by considering different noise levels. Gaussian white noise has been added to the output voltages of both the reference and the transducer under test. In particular, SNRs between 40 and 120 dB have been considered.

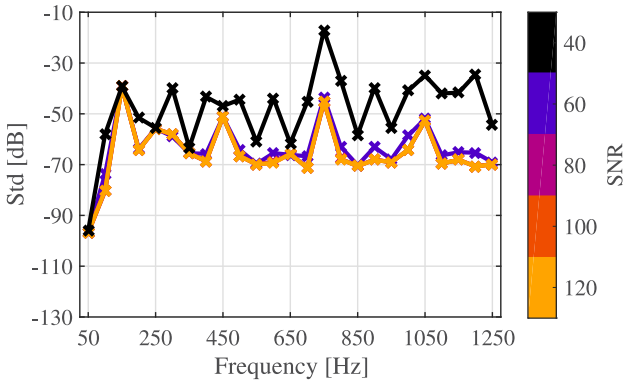

Fig. 4. Numerical simulations: total standard deviations of the BLA for different SNRs.

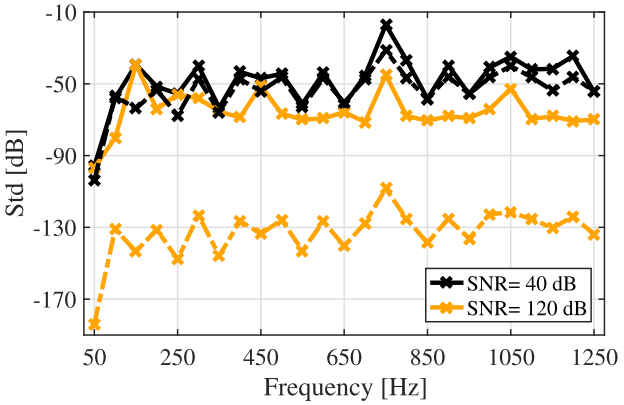

Fig. 5. Numerical simulations: total (solid line) and noise (dashed line) standard deviations considering maximum and minimum SNRs.

$M = 200$ multisine test signals with 50-Hz fundamental frequency have been generated; fundamental and harmonic amplitudes and phases have been obtained by sampling the previously introduced PDFs. $P = 50$ periods of each signal have been acquired. The procedure has been repeated for different SNRs; the $G_{\mathrm{BLA}}(jk\omega_0)$ and the sample variances have been estimated using (13), (19), and (20).

Increasing SNR leads to a (proportional) reduction of $s_{\mathrm{BLA},N}(jk\omega_0)$ over the whole frequency range. In fact, those standard deviations take into the account only the impact of noise on the variability of the estimate. The class of excitation signals employed for the characterization has a strong fundamental component and weak harmonics; for this reason, $s_{\mathrm{BLA},N}$ is considerably lower at the fundamental with respect to the harmonics.

On the other hand, the total sample standard deviation $s_{\mathrm{BLA}}(jk\omega_0)$ is affected both by noise and nonlinear stochastic effect (Fig. 4); therefore, it exhibits a completely different behavior. It should be noticed that by continuously increasing the SNR, $s_{\mathrm{BLA}}(jk\omega_0)$ diminishes but it approaches a lower bound that only depends on nonlinearity.

Fig. 5 reports the standard deviations evaluated considering the highest and lowest SNR. In the presence of a poor SNR,

TABLE III
VT SPECIFICATIONS

Primary voltage	200 V
Secondary voltage	100 V
Burden	20 VA
Accuracy class	0.5

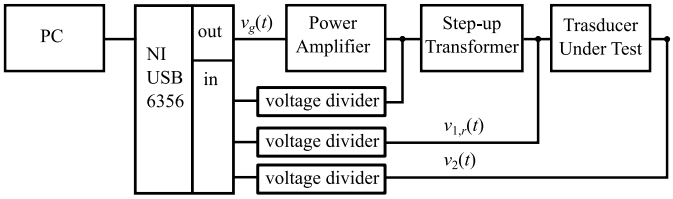

Fig. 6. Experimental setup.

TABLE IV
POWER AMPLIFIER SPECIFICATIONS

Maximum output voltage	140 V
Maximum voltage gain	50
-3dB bandwidth	5 Hz-50 kHz
SNR	>100 dB

noise may completely mask nonlinearity (black lines in Fig. 5). Except of few harmonics that are affected by strong nonlinear phenomena (e.g., the third and fifth), $s_{\mathrm{BLA},N}(jk\omega_0)$ is close to $s_{\mathrm{BLA}}(jk\omega_0)$. In order to detect and quantify nonlinearities, it is necessary to increase the measurement time or to improve the experimental setup, having assumed that the main source of noise is not the transducer under test. As the SNR is increased, $s_{\mathrm{BLA},N}(jk\omega_0)$ becomes smaller and well-separated from $s_{\mathrm{BLA}}(jk\omega_0)$ (tangerine lines in Fig. 5).

V. EXPERIMENTAL SETUP

The proposed approach has been applied to the characterization of a 200 V/100 V conventional VT, whose characteristics are reported in Table III.

The overall architecture of the experimental setup is depicted in Fig. 6. A National Instruments USB-6356 board connected to a PC has been employed to generate the excitation signals and to acquire the transducer input and output. The device is characterized by 16-bit resolution and simultaneous sampling with a maximum rate of 1.25 MHz. In order to apply the periodic, distorted excitation signals to the VT under test as required by the proposed method, the approach already employed in [10] and [11] has been adopted for the purpose. An analog output of the board has been connected to a power amplifier, whose specifications are listed in Table IV. Since its maximum output voltage is not sufficient to perform the tests, a 100 V/400 V transformer has been interposed between the amplifier and the transducer under test. The secondary winding of the instrument transformer to be characterized has been connected to its rated resistive burden.

The primary and secondary voltages of the transformer under test [$v_{1,r}(t)$ and $v_2(t)$, respectively] have been acquired

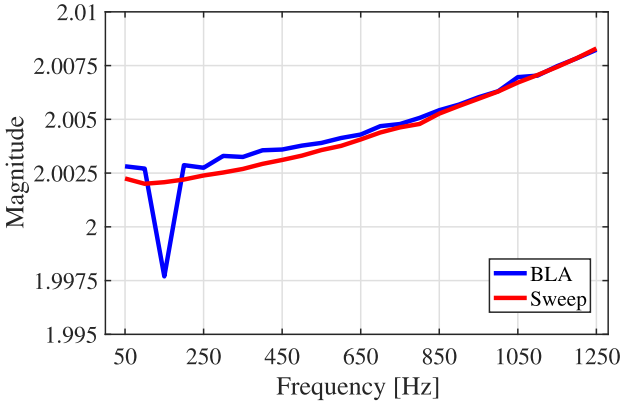

Fig. 7. Experimental results: BLA and single-tone FRF magnitude responses.

by means of resistive dividers connected to Analog Devices AD215BY isolation amplifiers in unity gain, noninverting configuration. These transducers have been calibrated over the whole considered frequency range. After calibration, the residual gain mismatch is below 1×10^{-4} with a phase shift lower than 0.2 mrad.

The power amplifier output voltage has been monitored by means of a wide bandwidth voltage probe in order to check that it remains within the rated capability. The signal generation, acquisition, and processing has been managed by means of a PC. A 100-kHz sampling rate has been employed; thanks to the synchronization between sampling and generation, spectra can be easily obtained by using the discrete Fourier transform without running into leakage artifacts.

VI. EXPERIMENTAL RESULTS

Estimating the BLA and its standard deviations requires injecting a set of excitation signals belonging to the class E as defined in Section IV-A in order to perform the characterization under realistic conditions. Because of the input–output characteristics of the power amplifier and of the step-up transformer, the voltage $v_{1,r}(t)$ applied to the transducer under test may be significantly different from a scaled replica of the generated signal $v_g(t)$. For this reason, before the tests, the small-signal FRF between $v_{1,r}(t)$ and $v_g(t)$ has been estimated by injecting a random phase multisine signal [24]. The obtained FRF can be employed to prefilter the desired excitation voltage waveform in order to compensate for the linear distortion introduced by the generation system. Of course, nonlinearities cannot be canceled. However, assuming that the power amplifier and the step-up transformer operate within their rated capabilities, nonlinear distortion just produces a slight change in the actual excitation signal.

In order to perform the characterization, first of all $M = 200$ excitation waveforms have been sampled from the class E and the corresponding voltages $v_g(t)$ to be generated have been obtained through prefiltering. Then, for each generic mth trial, $P = 100$ periods of $v_{1,r}(t)$ and $v_2(t)$ have been acquired. Once having collected the data from all the trials, the BLA can be estimated.

Fig. 7 shows the comparison between the magnitude of the BLA and the FRF obtained by applying single-tone voltages

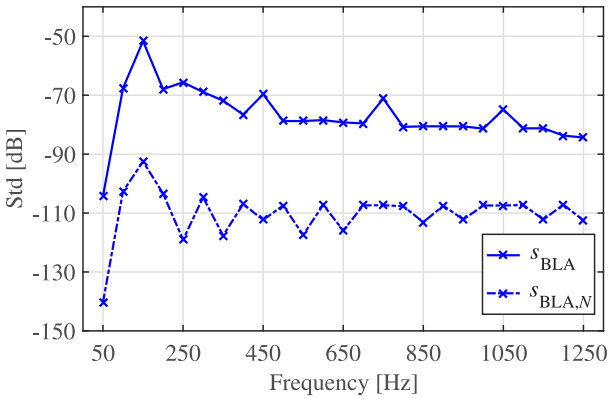

Fig. 8. Experimental results: BLA standard deviations.

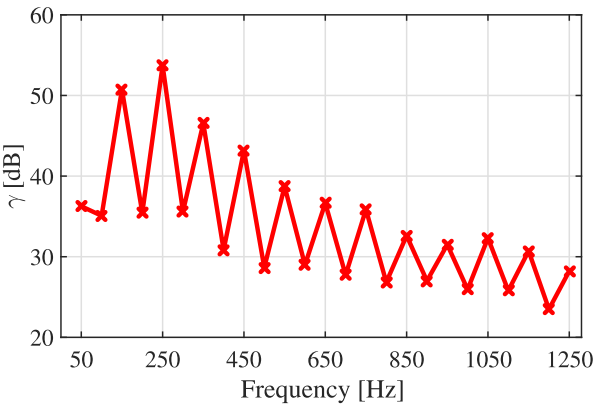

Fig. 9. Experimental results: ratios between total and noise standard deviations.

having the rated amplitude. The difference between the two estimates cannot be explained with the uncertainty of the measurement setup. Therefore, it is due to the systematic nonlinear contributions that are included in the BLA, but not considered by a conventional FRF measurement. From a practical point of view, the deviations are small, except at the third harmonic that appears to be the most affected by systematic nonlinearity. In this case, the FRF estimated by using the BLA approach is about 0.25% lower. It should be noticed that the difference between the two FRFs has a decreasing trend over frequency as nonlinearity is mostly related to the harmonic distortion produced by the fundamental term, which is, therefore, more relevant at low harmonic orders. Similar considerations apply when comparing the phase response of the BLA with that of the conventional FRF.

The total and sample standard deviations of the BLA described in Section III-C have been computed using (19) and (20); Fig. 8 shows their comparison. For every spectral component, the total sample standard deviation $s_{\mathrm{BLA}}(jk\omega_0)$ is much higher with respect to the noise $s_{\mathrm{BLA},N}(jk\omega_0)$. Therefore, the experimental results show that nonlinear stochastic contributions can be clearly distinguished from the noise floor, and most part of the total variance is due to nonlinearity. The 50-Hz component is characterized by very low sample and noise standard deviations. Therefore, nonlinearity is almost negligible at this frequency, and the impact of noise is reduced since most of the energy of the excitation signals is located at the fundamental.

As for the BLA estimation, it can be noticed that the 150-Hz component is the most affected by nonlinearity: the total standard deviation reaches the highest value at this frequency, namely, about -50 dB. Even harmonics are characterized by lower total standard deviations, although higher noise standard deviations. Other harmonics whose orders are odd multiples of three (9th, 15th, and 21st) show a significant total standard deviation with respect to the nearby ones.

These considerations also apply to the simulation results presented in Section IV (Fig. 4), and the reason is strongly related to the class of the excitation signals. First of all, nonlinearity of the instrument transformer is mostly odd (as expected, since it is due to core magnetization) and produced by the strong fundamental voltage (that provides the main contribution to core flux); thus, it mainly affects odd harmonics. Practical power systems are weakly unbalanced; therefore, harmonics whose orders are multiples of three are expected to be extremely small. In fact, amplitude limits for these components are very low, as from Table I [29]. Therefore, the impact of nonlinearity is magnified because of the small spectral content of the excitation signals at these components. Even harmonics are generally characterized by higher noise standard deviations since also in this case, the excitation signal is rather weak. In fact, even harmonics are expected to be very small (Table I, [29]).

In order to complete the analysis, a meaningful indicator is represented by the ratio $\gamma(jk\omega_0)$ between the two standard deviations

$$\gamma(jk\omega_0) = \frac{s_{\mathrm{BLA}}(jk\omega_0)}{s_{\mathrm{BLA},N}(jk\omega_0)}. \tag{22}$$

It quantifies the impact of stochastic nonlinear contributions with respect to noise; it corresponds to the distance between the two standard deviations when plotted in log scale (Fig. 9). As expected, all the odd harmonics show a larger $\gamma(jk\omega_0)$ since the transformer under test mostly suffers from odd nonlinearity.

The accuracy of the transducer under test can be evaluated in terms of relative TVE expressed as percentage of the voltage measured by the reference transducer. The relative TVE has been evaluated for each signal m and harmonic order k in two different cases: when the measured voltage is obtained from the output of the transducer under test by using the BLA, and when the 50-Hz ratio is employed. In order to synthetize the results, for each harmonic order, the TVE_{95}[%] has been computed for the two cases as the 95th percentiles of the relative TVEs. Results are shown in Fig. 10.

When using the BLA compensation, it is evident that the TVE_{95} is well below 0.5% (about 0.01%) for the fundamental term, but it is considerably higher for all the other components. Of course, the reason is due to nonlinear effects that cannot be compensated by using a simple gain and phase shift calibration. Even in this case, it should be noticed that the higher values occur for the low-order harmonics: the third is characterized by TVE_{95} above 3.8%. TVE values for components whose orders are multiple of three are increased by the weakness of the excitation. It should be noticed that using the single-tone FRF instead of the BLA would have

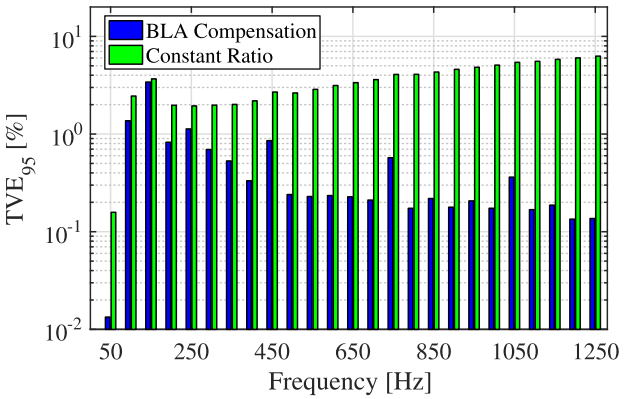

Fig. 10. Experimental results: TVE 95th percentiles.

resulted in very similar TVE_{95} values. The reason is that the difference between the conventional FRF and the BLA is almost completely masked by stochastic nonlinearities.

On the other hand, using a constant gain results in significantly greater errors for the high-order harmonics, where the linear amplitude and phase distortion introduced by the VT are larger. On the contrary, when looking at the 150-Hz component, the TVE_{95} is just slightly higher since most of the error is due to nonlinearity.

VII. Conclusion

It is well known that the behavior of voltage instrument transformers includes nonlinear effects that may have a significant impact on harmonic measurements. The effect of these small nonlinearities is magnified by the typical quasi-sinusoidal spectral content of the voltage waveforms in ac power systems. A systematic procedure to test voltage instrument transformers able to consider nonlinearities cannot be found in the scientific literature or in the standards. For this reason, the present paper proposes to apply the concept of BLA to the metrological characterization of voltage instrument transformers. For a given class of input signal, the BLA represents the FRF that allows the optimal reconstruction of the input voltage starting from the transducer output, thus guaranteeing the most accurate measurement. In order to achieve the best results, such class of excitation signals shall resemble the voltages measured by the instrument transformer during normal operation. Other than estimating the BLA, noise and the total standard deviations can be easily computed. The first measures the overall impact of noise on the BLA, while the second one includes also the effect of undermodeling; thus, stochastic nonlinearities cannot be included in the BLA. As a case study, the approach is applied to the characterization of a conventional inductive VT. Results show that nonlinearities significantly affect the measurement of low-order harmonics, while compensating the frequency response is effective only at the higher frequencies.

References

[1] *Electromagnetic Compatibility (EMC)—Part 4-7: Testing and Measurement Techniques—General Guide on Harmonics and Interharmonics Measurements and Instrumentation, for Power Supply Systems and Equipment Connected Thereto*, document BS EN 61000-4-7:2002+A1:2009, 2009.

[2] L. Peretto, E. Scala, and R. Tinarelli, "Design and characterization of an electric field based medium voltage transducer," in *Proc. IEEE Int. Instrum. Meas. Technol. Conf.*, Victoria, BC, Canada, May 2008, pp. 1617–1622.

[3] N. Locci, C. Muscas, and S. Sulis, "Experimental comparison of MV voltage transducers for power quality applications," in *Proc. IEEE Int. Instrum. Meas. Technol. Conf.*, Singapore, May 2013, pp. 92–97.

[4] L. Peretto, R. Sasdelli, E. Scala, and R. Tinarelli, "An equipment for voltage transducers calibration oriented to the uncertainty estimate in DSP-based measurements," in *Proc. IEEE Instrum. Meas. Technol. Conf.*, May 2005, pp. 597–602.

[5] M. Faifer, S. Toscani, and R. Ottoboni, "Electronic combined transformer for power-quality measurements in high-voltage systems," *IEEE Trans. Instrum. Meas.*, vol. 60, no. 6, pp. 2007–2013, Jun. 2011.

[6] G. Crotti, D. Gallo, D. Giordano, C. Landi, and M. Luiso, "A characterized method for the real-time compensation of power system measurement transducers," *IEEE Trans. Instrum. Meas.*, vol. 64, no. 6, pp. 1398–1404, Jun. 2015.

[7] M. Zucca, M. Modarres, D. Giordano, and G. Crotti, "Accurate numerical modelling of MV and HV resistive dividers," *IEEE Trans. Power Del.*, vol. 32, no. 3, pp. 1645–1652, Jun. 2017.

[8] *Instrument Transformers—Part 3: Additional Requirements for Inductive Voltage Transformers*, document IEC 61869-3:2011, 2011.

[9] *Instrument Transformers—Part 6: Additional General Requirements for Low-Power Instrument Transformers*, document IEC 61869-6:2016, 2016.

[10] M. Faifer, R. Ottoboni, S. Toscani, C. Cherbaucich, M. Gentili, and P. Mazza, "A medium voltage signal generator for the testing of voltage measurement transducers," in *Proc. IEEE Int. Instrum. Meas. Technol. Conf.*, Minneapolis, MN, USA, May 2013, pp. 194–199.

[11] M. Faifer, R. Ottoboni, S. Toscani, C. Cherbaucich, and P. Mazza, "Metrological characterization of a signal generator for the testing of medium-voltage measurement transducers," *IEEE Trans. Instrum. Meas.*, vol. 64, no. 7, pp. 1837–1846, Jul. 2015.

[12] *Instrument Transformers—The Use of Instrument Transformers for Power Quality Measurement*, document IEC TR 61869-103, 2012.

[13] R. Stiegler, J. Meyer, J. Kilter, and S. Konzelmann, "Assessment of voltage instrument transformers accuracy for harmonic measurements in transmission systems," in *Proc. IEEE Int. Conf. Harmon. Quality Power (ICHQP)*, Belo Horizonte, Brazil, Oct. 2016, pp. 152–157.

[14] M. Klatt, J. Meyer, M. Elst, and P. Schegner, "Frequency Responses of MV voltage transformers in the range of 50 Hz to 10 kHz," in *Proc. Int. Conf. Harmon. Quality Power*, Bergamo, Italy, 2010, pp. 1–6.

[15] D. A. Douglass, "Potential transformer accuracy at 60 HZ voltages above and below rating and at frequencies above 60 HZ," *IEEE Trans. Power App. Syst.*, vol. PAS-100, no. 3, pp. 1370–1375, Mar. 1981.

[16] S. Zhao, H. Y. Li, P. Crossley, and F. Ghassemi, "Testing and modelling of voltage transformer for high order harmonic measurement," in *Proc. Int. Conf. Electr. Utility Dereg. Restruct. Power Technol.*, Weihai, China, 2011, pp. 229–233.

[17] G. Crotti, D. Gallo, D. Giordano, C. Landi, M. Luiso, and M. Modarres, "Frequency response of MV voltage transformer under actual waveforms," *IEEE Trans. Instrum. Meas.*, vol. 66, no. 6, pp. 1146–1154, Jun. 2017.

[18] T. Lei *et al.*, "Behavior of voltage transformers under distorted conditions," in *Proc. IEEE Int. Instrum. Meas. Technol. Conf.*, Taipei, Taiwan, May 2016, pp. 1–6.

[19] M. Schetzen, *The Volterra and Wiener Theories of Nonlinear Systems*. Hoboken, NJ, USA: Wiley, 2006.

[20] W. J. Rugh, II, *Nonlinear System Theory: The Volterra/Wiener Approach*. Baltimore, MD, USA: The Johns Hopkins Univ. Press, 1981.

[21] M. Faifer, R. Ottoboni, M. Prioli, and S. Toscani, "Simplified modeling and identification of nonlinear systems under quasi-sinusoidal conditions," *IEEE Trans. Instrum. Meas.*, vol. 65, no. 6, pp. 1508–1515, Jun. 2016.

[22] M. Faifer, C. Laurano, R. Ottoboni, M. Prioli, S. Toscani, and M. Zanoni, "Definition of Simplified frequency-domain volterra models with quasi-sinusoidal input," *IEEE Trans. Circuits Syst. I, Reg. Papers*, to be published.

[23] M. Faifer, C. Laurano, R. Ottoboni, S. Toscani, and M. Zanoni, "Voltage transducers testing procedure based on the best linear approximation," in *Proc. IEEE Int. Workshop Appl. Meas. Power Syst.*, Liverpool, U.K., Sep. 2017, pp. 31–36.

[24] R. Pintelon and J. Schoukens, *System Identification: A Frequency Domain Approach*, 2nd ed. Boston, MA, USA: Wiley, 2012.

[25] J. Schoukens, T. Dobrowiecki, and R. Pintelon, "Parametric and nonparametric identification of linear systems in the presence of nonlinear distortions—A frequency domain approach," *IEEE Trans. Autom. Control*, vol. 43, no. 2, pp. 176–190, Feb. 1998.
[26] J. Schoukens, R. Pintelon, T. Dobrowiecki, and Y. Rolain, "Identification of linear systems with nonlinear distortions," *Automatica*, vol. 41, no. 3, pp. 491–504, 2005.
[27] A. E. Nordsjö and T. Wigren, "On estimation of errors caused by nonlinear undermodelling in system identification," *Int. J. Control*, vol. 75, no. 14, pp. 1100–1113, 2002.
[28] J. Schoukens, K. Barbé, L. Vanbeylen, and R. Pintelon, "Nonlinear induced variance of frequency response function measurements," *IEEE Trans. Instrum. Meas.*, vol. 59, no. 9, pp. 2468–2474, Sep. 2010.
[29] *Voltage Characteristics of Electricity Supplied by Public Distribution Networks*, Standard EN 50160, 2010.
[30] *Testing and Measurement Techniques—Power Quality Measurement Methods*, Standard IEC 61000-4-30, 2015.